Analysis of Surfaces from the LDEF A0114 - Phase II

Semi-Annual Report on Grant NAG1-1228

for the reporting period Mar. 1, 1991 - Aug. 31, 1991

Dr. John C. Gregory, Principal Investigator
Department of Chemistry
Materials Science Building, Room 111
The University of Alabama in Huntsville
Huntsville, Alabama 35899

John C. Gregory
NAG1-1228
10/15/91

During the above mentioned reporting period, work has concentrated on profilometry measurements of eroded and corroded sample surfaces, optical transmission measurements, analysis of the pinhole camera and XPS analysis of some samples. The following papers have appeared or been accepted for publication:

1) "Observation of ^{7}Be on the Surface of LDEF Spacecraft". Fishman, G.J., Harmon, B.A., Gregory, J.C., Parnell, T.A., Peters, P., Phillips, G.W., King, S.E., August, R.A., Ritter, J.C., Cutchin, J.H., Haskins, P.S., McKisson, J.E., Ely, D.W., Weisenberger, A.G., Piercey, R.B., and Dybler, T.: Nature, 349, 1991, pp678-680.

2) "Measurement of the Passive Attitude Control Performance of a Recovered Spacecraft", Gregory, J.C., and Peters, P.N.: Journal of Guidance, Control and Dynamics, AIAA, Accepted for publication, November, 1991.

3) "Effects on LDEF Exposed Copper Film and Bulk", J. C. Gregory, L.C. Christl, G.N. Raikar and P.N. Peters,, Proceedings of the LDEF First Post-Retrieval Symposium, Orlando, FL, June, 1991.

4) "Measurements of Erosion Characteristics for Metal and Polymer Surfaces Using Profilometry", J. C. Gregory, L.C. Christl and P.N. Peters, Proceedings of the LDEF First Post-retrieval Symposium, Orlando, Florida, June, 1991.

5) "The Interactions of Atmospheric Cosmogenic Radionuclides with Spacecraft Surfaces", J.C. Gregory, G.J. Fishman, A. Harmon, and T.A. Parnell, Proceedings of the LDEF First Post-retrieval Symposium, Orlando, Florida, June, 1991.

6) "Pinhole Cameras as Sensors for Atomic Oxygen in Orbit: Application to Attitude Determination of the LDEF", J.C. Gregory and P.N. Peters, Proceedings of the LDEF First Post-retrieval Symposium, Orlando, Florida, June, 1991.

7) "Interaction of Atomic Oxygen with Solid Surfaces in Low Earth Orbit: Results from LDEF Experiment A0114", J.C. Gregory, Paper presented at the Fifth International Symposium on Materials in a Space Environment, Mandelieu-Cannes, France, September 16-20, 1991.

THE INTERACTIONS OF ATMOSPHERIC COSMOGENIC RADIONUCLIDES WITH SPACECRAFT SURFACES

J. C. Gregory
The University of Alabama in Huntsville
Materials Science Building Room 111
Huntsville, Alabama 35899
Phone: 205/895-6028, Fax: 205/895-6819

G.J. Fishman, B. A. Harmon, T.A. Parnell
NASA Marshall Space Flight Center
Space Science Laboratory ES-62
Huntsville, AL 35812
Phone: 205/544-7690, Fax: 205/544-7754

SUMMARY

The discovery of the cosmogenic radionuclide ^{7}Be on the front surface (and the front surface only) of the LDEF spacecraft (ref. 1) has opened opportunities to investigate new phenomena in several disciplines of space science. Our experiments have shown that the ^{7}Be found was concentrated in a thin surface layer of spacecraft material. We are able to explain our results only if the source of the isotope is the atmosphere through which the spacecraft passed. We should expect that the uptake of beryllium in such circumstances will depend on the chemical form of the Be and the chemical nature of the substrate. We have found that the observed concentration of ^{7}Be does, in fact, differ between metal surfaces and organic surfaces such as PTFE (Teflon). We note however that (a) organic surfaces, even PTFE, are etched by the atomic oxygen found under these orbital conditions, and (b) the relative velocity of the species is 8 $km^{-1}s$ relative to the surface and the interaction chemistry and physics may differ from the norm.

^{7}Be is formed by spallation of O and N nuclei under cosmic ray proton bombardment. The principal source region is at altitudes of 12-15 km. While very small quantities are produced above 300km, the amount measured on LDEF was 3 to 4 orders of magnitude higher than expected from production at orbital attitude. The most reasonable explanation is that ^{7}Be is rapidly transported from low altitudes by some unknown mechanism. The process must take place on a time scale similar to the half-life of the isotope (53 days).

Many other isotopes are produced by cosmic ray reactions, and some of these are suited to measurement by the extremely sensitive methods of accelerator mass spectrometry. We have begun a program to search for these and hope that such studies will provide new methods for studying vertical mixing in the upper atmosphere.

INTRODUCTION

The LDEF spacecraft was launched by the space shuttle Challenger on 7 April 1984 into a nearly circular orbit with an inclination of 28.5° and an altitude of 480 km. It was retrieved by the space shuttle Columbia on 12 January 1990 at an altitude of 310 km. Because of its large mass, long space exposure and the wide variety of materials onboard, the LDEF provided a unique opportunity for induced radioactivity studies. These measurements are still in progress and will be reported elsewhere.

The LDEF spacecraft has a twelve-sided cylindrical aluminium structure, 9.1 m long by 4.3 m in diameter (see Fig. 1). Its structure consisted of an open grid to which were attached various experiment trays designed to measure the effects of long space exposure on spacecraft materials and components. Throughout its orbital lifetime, the spacecraft was passively stabilized about all three axes of rotation, allowing one end of the spacecraft to point always toward the Earth, and fixed leading and trailing with respect to the orbital motion.

After its return to the Kennedy Space Center, gamma ray spectra were obtained along each of the 12 sides of the spacecraft using a germanium detector array provided by the Naval Research Laboratory. The gamma-ray line at 478 keV from the radioactive decay of ^{7}Be was observed to emanate strongly from the leading side of the spacecraft. (ref. 2) The weaker signal observed from the trailing side of the spacecraft was later traced to the gamma-ray flux from the leading surfaces after attenuation from passing through the body of the LDEF.

EXPERIMENTAL MEASUREMENTS OF RADIOACTIVITY

Individual components were brought to the Marshall Space Flight Center to quantify the residual radioactivity on the LDEF. Much of the counting work was performed at other radiation laboratories around the country. The authors are particularly indebted to Dr. Charles Frederick of the TVA Western Area Radiation Laboratory, Muscle Shoals, Alabama for many of the Al clamp plate assays. A high-purity germanium detector inside a low-level background facility was used to obtain spectra of small aluminium and steel samples taken from the leading and trailing sides. In Figs 2 and 3, gamma-ray spectra of two identical aluminium plates and two steel trunnion end pieces taken from the leading and trailing sides of the spacecraft are shown. A clear ^{7}Be gamma ray signal was seen on materials from the leading side, with little or no signal above background on the trailing side.

In Figure 4 the ^{7}Be activities for aluminum tray-clamps taken from trays all round the LDEF are shown, clearly demonstrating the leading edge effect. While ^{7}Be is also produced by spallation of Al nuclei in the spacecraft by cosmic rays, first order calculations have shown it to be barely measurable. Also the known anisotropy of the cosmic ray flux (the east-west effect) should have resulted in higher production on the rear (west-facing side) of the LDEF. Another isotope ^{22}Na, produced by spallation of spacecraft Al, clearly shows higher activity on the trailing edge of the satellite. Figure 5 shows tray clamp activities of ^{22}Na about twice as high on the trailing as on the leading edge, in agreement with the east-west anisotropy of the cosmic rays and trapped protons. This evidence clearly pointed to a source of ^{7}Be in the atmosphere being swept up by the front surface of the spacecraft.

In Table 1, the measured number of ^{7}Be atoms per unit area on various spacecraft surfaces is shown. The results are corrected to the retrieval date of 12 January 1990 and for the offset angle from the leading direction. The areal density for ^{7}Be on the aluminium and steel is the same within the experimental uncertainty, and is apparently not a strong function of the type or surface condition of the metal. However, the Teflon thermal coating which was used on many LDEF experiment trays, has a density of ^{7}Be an order of magnitude lower than that found on the aluminum surface. The reason for this apparent difference in uptake efficiency is unknown, but could be related to the covalent-bond structure of the material. The explanation may be complicated, also, by the observed erosion of the Teflon surface by atomic oxygen.

TABLE 1

LDEF Be-7 Surface Concentrations*

Material	Be-7 Areal Density (x 10e5 atoms/cm2)
Stainless steel trunnion face	5.3 +- 0.7
Polished aluminum plate- Exp. A0114	6.7 +- 1.0
Anodized aluminum experiment tray clamp	4.6 +- 0.5
Teflon thermal cover	0.9 +- 0.2

* Corrected for decay since recovery and for surface orientation relative to spacecraft ram direction.

^{7}Be PRODUCTION, DECAY AND DYNAMICS IN THE ATMOSPHERE

The short-lived isotope ^{7}Be was first detected in the atmosphere by Arnold and Al-Salih in 1955, (ref. 3) and later mapped by others as a function of altitude and latitude (ref. 4-8). It is produced in the atmosphere by high-energy cosmic-ray interactions with air as are other radioisotopes such as ^{14}C and ^{3}H. Once formed, ^{7}Be ions are presumed to oxidize rapidly and attach to small aerosol particles, which provide a downward transport mechanism from peak production regions of the atmosphere (ref. 9-16). The primary removal process for ^{7}Be, which occurs on a timescale comparable to its half-life, 53.2 days, is the washout of the aerosol-attached ^{7}Be in rain water (ref. 3-6).

At a given latitude above ~20 km, the production rate of ^{7}Be varies vertically and directly in proportion to the oxygen-nitrogen gas density. Peak production per unit volume occurs in the lower stratosphere, at 12-15 km, below which the cosmic-ray flux is substantially attenuated. At higher altitudes, the number of ^{7}Be atoms produced per unit volume decreases rapidly, but the number of ^{7}Be atoms produced per unit mass of air is essentially constant. Balloon and aircraft measurements (ref. 6, 15) are in approximate agreement with this, although few measurements extend much above the peak production altitudes.

From the measured densities of ^{7}Be on LDEF surfaces and in making some simplifying assumptions, we can estimate the concentration of ^{7}Be atoms per cm^3 of air at the LDEF orbital

altitude. Since the lifetime of LDEF is much greater than the mean lifetime of a ^{7}Be atom, and ignoring changes in altitude over the last 6 months in orbit, we assume a steady state relationship between pick-up of ^{7}Be and loss by decay:

$$\frac{dn}{dt} = 0 = -k\ n_{eq} + n^*\ v\ p_s$$

where: n is the density of ^{7}Be atoms on the surface at time t
k is the first-order decay constant for ^{7}Be
n_{eq} is the steady-state surface density of ^{7}Be in atoms cm^{-2}
n^* is the concentration of ^{7}Be atoms in orbital space (atoms cm^{-3})
v is the spacecraft velocity (cm)(s^{-1})
p_s is the sticking probability of Be on a metal surface

for first order kinetics of radioactive decay:

$$k = \frac{\ln 2}{t_{1/2}}$$

where: $t_{1/2}$ is the half life

Thus we have:

$$n_{eq} = n^*\ v\ t_{mean}\ p_s$$

where $t_{mean} = \frac{t_{1/2}}{\ln 2} = 76.8$ days for ^{7}Be

From the measured value of n_{eq}, assuming $p_s = 1$,

we have $n^* = 1.2 \times 10^{-7}$ cm^{-3} at 320km

or a relative concentration of 3.8×10^6 atoms per gram of air. In the peak production region, below 20km, previous measurements (ref. 4-8) yield a concentration of 1000 ^{7}Be atoms per gram of air, or ~0.1 atoms cm^{-3}, in agreement with a simple calculation using known values of the cosmic-ray flux and the production cross-section for the isotope. Thus, the measured concentration of ^{7}Be per unit mass of air at 320km is three to four orders of magnitude greater than it would be if it had been produced at that altitude.

The simplest explanation is that Be is quickly transported upwards from regions of the atmosphere where its numerical concentration is much higher (but not its relative concentration with respect to oxygen and nitrogen). This transport must take place on time scales similar to or shorter than the radioactive half-life (53.2 days).

Vertical transport timescales at altitudes of several tens of km to 100km are considered to be too long to provide an efficient source, but Petty (ref. 17) has shown that above a certain altitude (not well defined, but about 100km) simple diffusion of the light nucleus in the Earth's gravitational field would provide an enrichment of a factor of 500 or more at 300km. Turbulent mixing below 100km cannot be easily invoked as it proceeds at times scales longer than the isotope half-life. More detailed calculations are needed to see if closer agreement can be reached.

ATMOSPHERIC CHEMISTRY AND SURFACE CHEMISTRY OF Be

Thus far we have considered the chemical form of Be to be single atoms of mass 7. At low altitudes, rapid oxidation would be expected and in regions close to the tropopause, this would be followed by rapid absorption onto aerosol particles. The raining-out of these Be-bearing aerosols has proved a useful tool for measuring the efficiency of tropospheric mixing by thunderstorms.

If the Be were in the form of its normal oxide BeO (mass 23) at altitudes above 100 km, we can no longer rely on rapid diffusion to higher altitudes. While not much appears to be known of Be chemistry in the upper atmosphere, a great deal of work has been done on the chemistry of metals ablated into the upper atmosphere from meteorites. These metals include Mg, Ca, Al, Si and Fe.

^{7}Be is formed as a "hot" atom or ion, which must rapidly thermalize with the atmosphere. From studies of meteoritic ions in the atmosphere we may draw some general conclusion as to the chemical form in which the Be atom will finally take. The form of the meteoritic ions is highly variable with altitude and between day and night. Electropositive metals readily form positive ions:

$$Fe + h\nu \rightarrow Fe^{+} + e$$
$$Fe + O_2^{+} \rightarrow Fe^{+} + O_2$$

At low altitudes neutralization may occur (X is a third molecule):

$$Fe^{+} O_2 + X \rightarrow FeO_2^{+} + X$$
$$FeO_2^{+} + e \rightarrow Fe + O_2$$

In general at altitudes in excess of 100km the metal (M) oxides cannot survive in appreciable quantities due to reactions such as

$$MO^{+} + h\nu \rightarrow M^{+} + O$$
and $$MO^{+} + O \rightarrow M^{+} + O_2$$

Thus at higher altitudes the singly-charged positive ion dominates for most metallic species studied. Of interest is the ratio M^{+}/M which varies with altitude and electropositive character of the metal. Examples of some measured ratios from the literature (ref. 18) for silicon and iron are:

Si^{+}/Si	=	0.006 at 96km
		0.2 at 110km
Fe^{+}/Fe	=	5 at 100km
		220 at 110km

Thus above 150km (and perhaps as low as 100km) most Be should exist as Be^{+}.

Important reactions might be:

$$Be + h\nu \rightarrow Be^{+} + e$$
$$BeO + O_2^{+} \rightarrow BeO^{+} + O_2$$
$$BeO + h\nu \rightarrow BeO^{+} + e$$
$$BeO^{+} + O \rightarrow Be^{+} + O_2$$

It is reasonable that a positive metal ion striking a clean metal oxide surface, especially with several eV kinetic energy, should easily enter the oxide lattice and remain trapped. While most metal (and metal oxide) surfaces in the ground-level atmosphere are usually found (by ESCA techniques) to be covered with a layer of hydrocarbon contamination, this is not the case with the leading surfaces of LDEF which are known to be continuously cleaned of combustible material by the action of atomic oxygen in the atmosphere. These atomic oxygen/satellite surface interactions have been intensively studied on the LDEF. The interaction of Be ions with metal oxides is an example of a new kind of chemical reaction between atmospheric species and satellite surfaces and has implications yet to be explored.

We investigated the form of binding of the Be to the aluminium surfaces on LDEF. Possibilities included (1) binding within an adsorbed contaminant layer, for example of hydrocarbon; (2) binding of Be-containing particulates, perhaps aerosols or meteoritic debris and (3) binding within the native oxide found on aluminum and other metals. Two kinds of Al plates from the LDEF were measured, some with several microns of oxide produced by anodization and the second type a polished Al plate from the UAH Atomic Oxygen Experiment A0114 (ref. 19). The oxide on this was only expected (ref.20) to be 50 - 100 Å thick.

The polished Al plate was coated with a solution of Collodion, which was then dried, stripped off and counted. No Be activity could be associated with the Collodion film. The method is used in industry to reliably and quantitatively remove particulates from sensitive surfaces. Next the plate was wiped first with alcohol, then with xylene. No activity was removed with the wipes. Finally an acid etch was used to remove the top 10 microns of the surface. The etch solution contained most of the Be activity formerly on the plate: that remaining being associated with either unetched surface or with re-adsorption of Be^{2+} ions onto the Al. This might be expected since a stable Be carrier solution was not used. The experimental results are consistent with the hypothesis that the Be species were penetrating the aluminium oxide layer on the surface of the plates and becoming permanently fixed in the oxide lattice. We believe the penetration to be of the order of one nanometer, since the kinetic energy of the Be species relative to the spacecraft was only 2.5eV. We do not have the capability to remove such a thin layer from large areas of metal surfaces, and thus cannot measure a depth/composition profile for the species.

^{7}Be is not the only nucleus produced by cosmic rays in the atmosphere. In fact all stable nuclei of lesser atomic weight than oxygen, nitrogen and argon must be formed. The means to detect the extremely small concentrations of most of these nuclides (in the presence of naturally occurring levels) do not exist. A few other unstable nuclides exist however with half-lives long enough to allow measurement, and short enough that there is no other natural background concentration. These are ^{14}C, ^{10}Be and possibly ^{26}Al (from argon).

The only method sensitive enough to measure these nuclides is accelerator mass spectrometry (AMS) (ref. 21). While the method has proved most useful for radioactive nuclei, emission of radiation by decaying nuclei is irrelevant to the AMS technique. Rather, all atoms of the nuclide are counted in the mass-spectrometer, giving some major advantages over radiation-counting methods.

^{10}Be is produced in a similar manner to ^{7}Be, by spallation of N and O induced by secondary neutrons from cosmic ray interactions in the atmosphere. The production efficiency is about 0.5 that of ^{7}Be, however its half-life is 1.5×10^{6} yrs (compared with 53.2d for ^{7}Be), resulting in measured ratios $^{10}Be/^{7}Be$ of about 3 in the stratosphere (ref. 22). While the atmospheric chemistry of the two isotopes should not differ appreciably, the diffusion of neutral atoms to higher altitudes should show measurable differences because of atomic mass.

^{10}Be decays to ^{10}B by internal conversion, emitting electrons over a wide energy range, while ^{7}Be decays to ^{7}Li by electron-capture, emitting gamma-rays of very narrow energy

distribution. The latter allows rates of a few decays per day to be measured in our low-level counting apparatus, while the former poses insurmountable counting problems. AMS however can detect ^{10}Be with undiminished sensitivity. We are currently working on chemical separation techniques (ref. 23) and plan a ^{10}Be run at the University of Pennsylvania (ref. 24) in fall of 1991.

We also plan a search for another cosmogenic radioisotope, ^{14}C, also using AMS. We plan to use the NSF-Arizona facility (ref. 25) to investigate the take up of ^{14}C species by blanket material from LDEF. Carbon chemistry is completely different from that of the metals. Cosmogenic carbon should form CO and CO_2 rapidly in the lower atmosphere but its behavior at higher altitudes is unknown. Upwards diffusion of the oxide species would not be favored (their masses are 28 and 44) and the adsorption on spacecraft materials is unknown.

REFERENCES

1. Fishman, G.J., Harmon, B.A., Gregory, J.C., Parnell, T.A., Peters, P., Phillips, G.W., King, S.E., August, R.A., Ritter, J.C., Cutchin, J.H., Haskins, P.S., McKisson, J.E., Ely, D.W., Weisenberger, A.G., Piercey, R.B., and Dybler, T. *Nature*, **349**, 678-680, (1991).

2. Phillips, G.W., King, S.E., August, R.A., Ritter, J.C., Cutchin, J.H., Haskins, P.S., McKisson, J.E., Ely, D.W., Weisenberger, A.G., Piercey, R.B., and Dybler, T: Gamma Radiation Survey of the LDEF Spacecraft. NASA, Proceedings of the First LDEF Post-Retrieval Symposium, Kissimmee, FL, June, 1991.

3. Arnold, J.R. & Al-Salih, H. *Science* **121**, 451 (1955).

4. Beniof, P.A. *Phys. Rev.* **104**, 1122-1130 (1956).

5. Lal, D., Malhotra, P.K. & Peters, B. *J. Atmos. Terr. Phys.* **12**, 306-328 (1958).

6. Lal, D. & Peters, B. *Encyclopedia of Physics* (ed. Sitte, K.) 46/2, 551-612 (Springer, New York, 1967).

7. Bhandari, N*J. Geophys. Res.* **75**, 2927-2930 (1970).

8. O'Brien, K. *J. Geophys. Res.***84**, 423-431 (1979).

9. Shapiro, M.H. & Forbes-Resha, J.L. *J. Geophys. Res.* **81**, 2647-2649 (1976).

10. Husain, L., Coffey, P.E., Meyers, R.E. & Cederwall, R.T. *Geophys. Res. Lett.* **4**, 363-365 (1977).

11. Bleichrodt, J.F. *J. Geophys. Res.* **83**, 3058-3062 (1978).

12. Viezee, W. & Singh, H.B. *Geophys. Res. Lett.* **7**, 805-88 (1980).

13. Raisbeck, G.M. *et al. Geophys. Res. Lett.* **8**, 1015-1018 (1981).

14. Sanak, J., Lambert, G. & Ardouin, B. *Tellus* **37B**, 109-115 (1985).

15. Dutkiewicz, V.A. & Husain, L. *J. Geophys. Res.* **90**, 5783-5788 (1985).

16. Dibb, J.E. *J. Geophys. Res.* **94**, 2261-2265 (1989).

17. Petty, G.W. *Geophys. Res. Lett.* **18** (**9**), p1687-1690 (Sept. 1991)

18. Solomon, S., Ferguson, E.E., Fahey, D.W. & Grutzen, P.J. *Planet. Space Sci.* **30** (11) 1117, (1982)

19. Gregory, J.C. and Peters, P.N., *The Long Duration Exposure Facility (LDEF)* NASA Publication **SP 473**, Edited by L.G. Clark, et al, pp 14-18, (1984).

20. Gregory, J.C., Peters, P.N., and Swann, J., *Applied Optics* **25**, 1290 (1986)

21. Elmore, D. and Phillips, F.M., *Science* **236**, 543, (1987)

22. McHargue, L.R. & Damon, P.E., *Reviews of Geophysics* 29 (2), p 141-158, May, 1991

23. Herzog, G.F. and Albrecht, A., Rutgers University, Dept. of Chemistry, Wright-Rieman Laboratory, New Brunswick, NJ, 08901, personal communications.

24. Klein, J. and Middleton, R., University of Pennsylvania, Dept. of Physics, David Rittenhouse Lab, Room 1N12, 209 South 33rd St., Philadelphia, PA 19104-6396, personal communications

25. Jull, A.J.T., University of Arizona, NSF-Arizona Accelerator Facility, Tuscon, Arizona 85721, personal communications

Figure 1. The LDEF spacecraft, showing the location of pieces of material studied for induced radio-activity

Figure 2. Portion of the gamma-ray spectrum obtained from an aluminum plate (a) on the leading side and (b) on the trailing side of the LDEF. The ^{7}Be line at 478 keV is seen only on the leading side.

Figure 3. Portion of the gamma-ray spectrum taken from the stainless steel trunnion (a) on the leading side and (b) on the trailing side of the LDEF. The ^{7}Be line is seen only on the leading side, whereas the spallation products produced within the steel itself, ^{54}Mn and ^{22}Na are seen on both trunnions.

Figure 4. ^{7}Be activities for aluminum tray-clamps taken from all round the LDEF. The leading edge is nominally 0 deg and the trailing edge 180 deg. ^{7}Be activity is clearly a function of surface area projected in the forward direction of the spacecraft.

Figure 5. ^{22}Na activities for aluminum tray clamps taken from around the LDEF. The leading edge is 0 deg. and the trailing edge 180 deg. Activity is peaked at the trailing edge but found all round the spacecraft. As expected from the anisotropic cosmic ray and trapped proton fluxes, more activity is induced in materials on the westerly (trailing) side of the spacecraft.

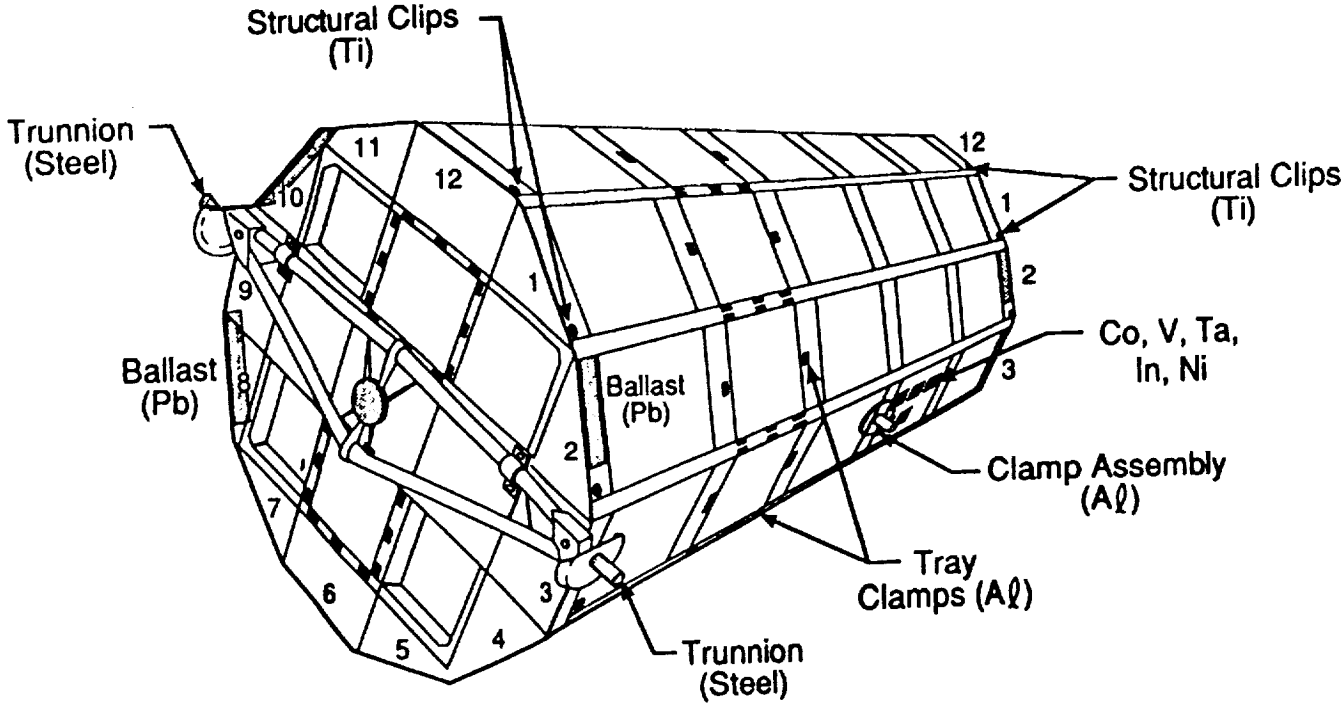

Figure 1. The LDEF spacecraft, showing the location of pieces of material studied for induced radio-activity

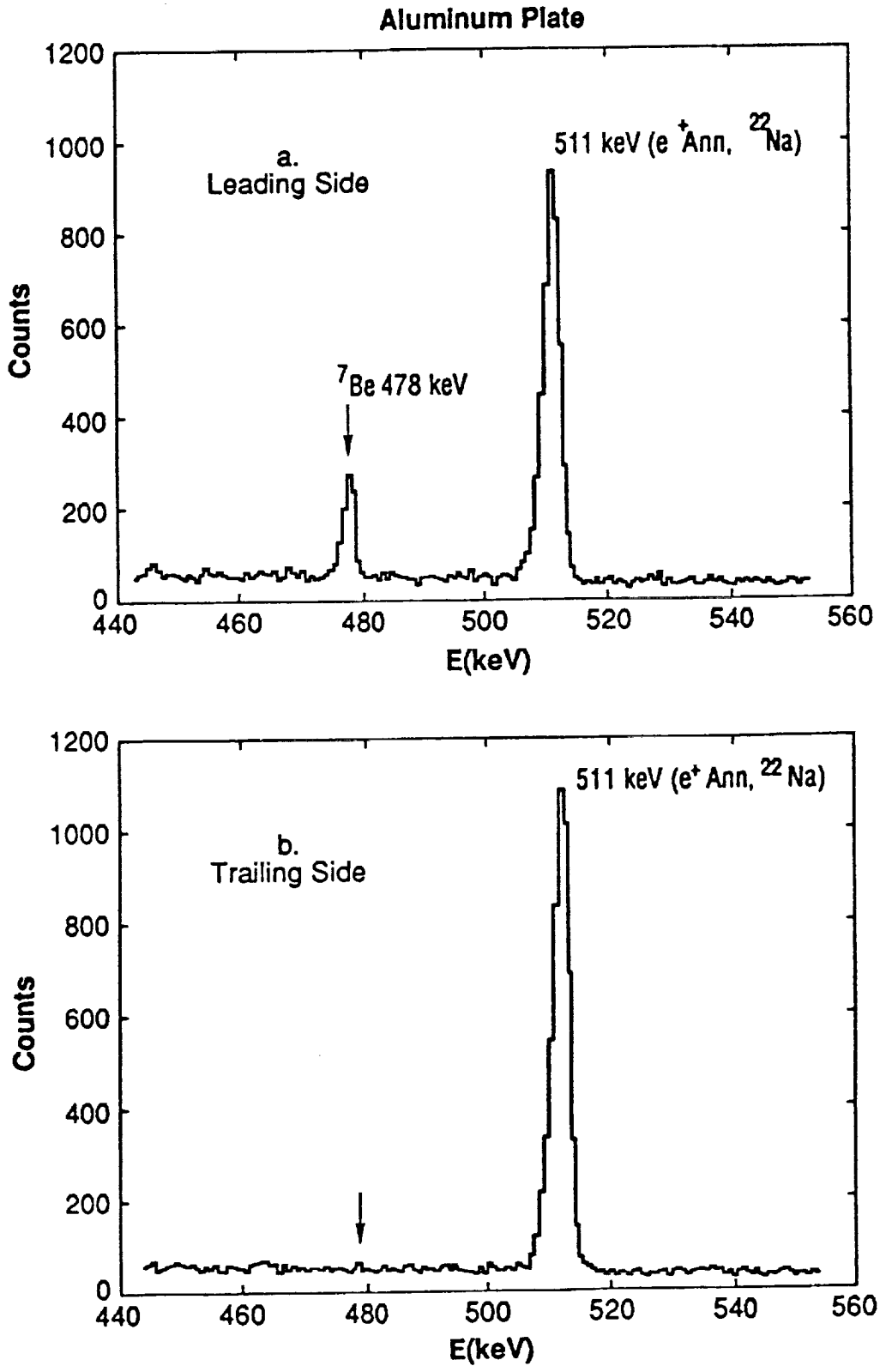

Figure 2. Portion of the gamma-ray spectrum obtained from an aluminum plate (a) on the leading side and (b) on the trailing side of the LDEF. The ^{7}Be line at 478 keV is seen only on the leading side.

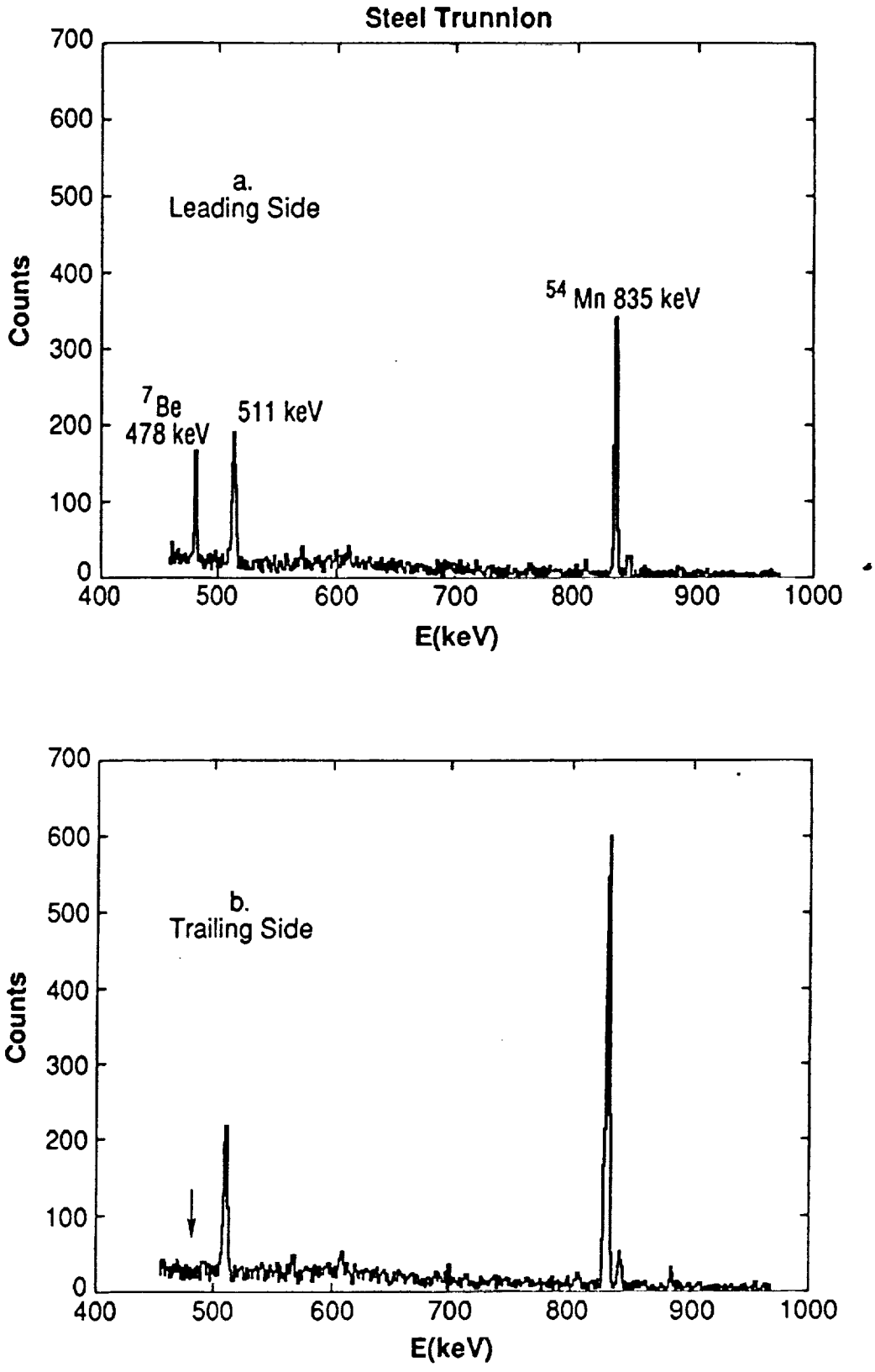

Figure 3. Portion of the gamma-ray spectrum taken from the stainless steel trunnion (a) on the leading side and (b) on the trailing side of the LDEF. The ^{7}Be line is seen only on the leading side, whereas the spallation products produced within the steel itself, ^{54}Mn and ^{22}Na are seen on both trunnions.

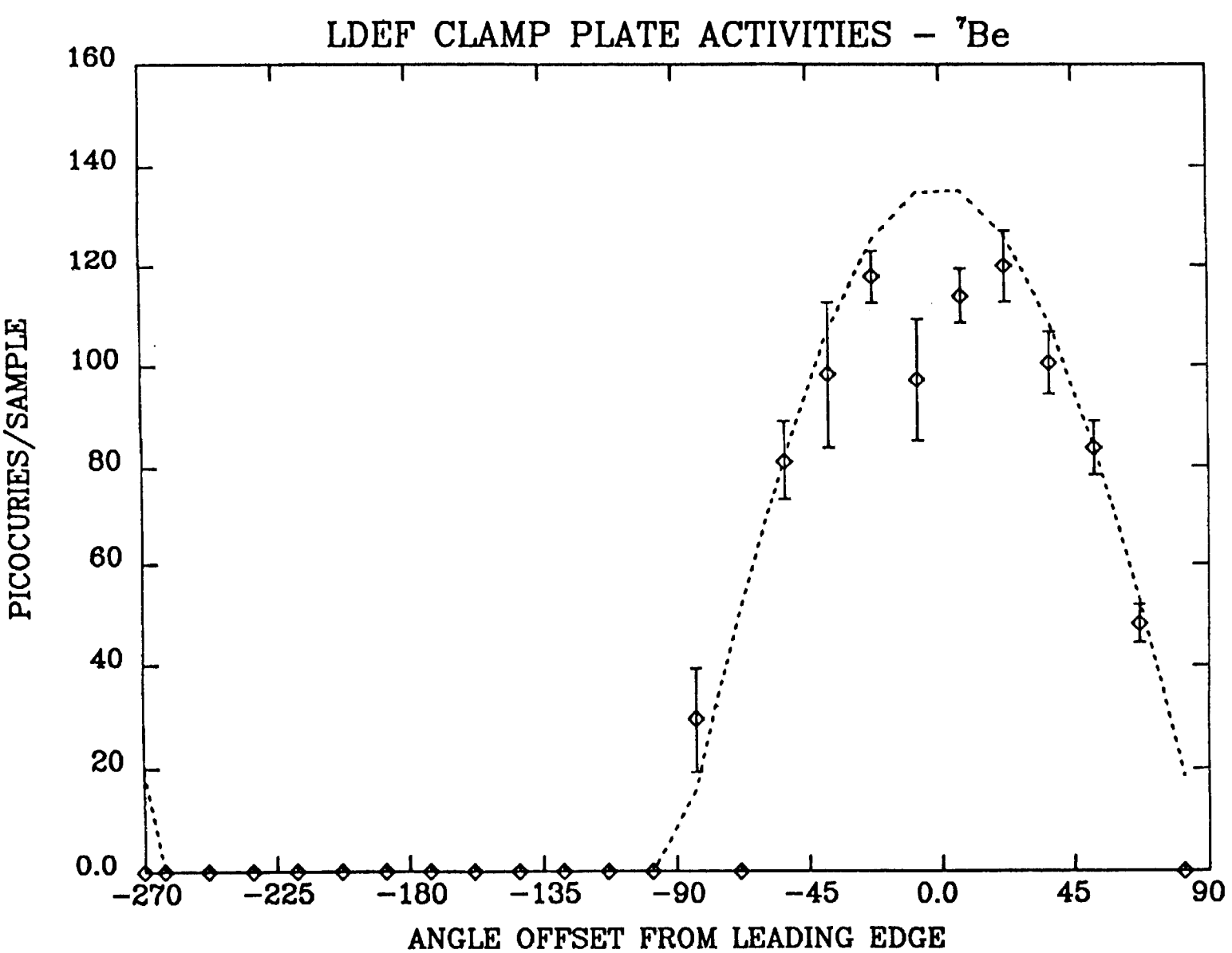

Figure 4. ^{7}Be activities for aluminum tray-clamps taken from all round the LDEF. The leading edge is nominally 0 deg and the trailing edge 180 deg. ^{7}Be activity is clearly a function of surface area projected in the forward direction of the spacecraft.

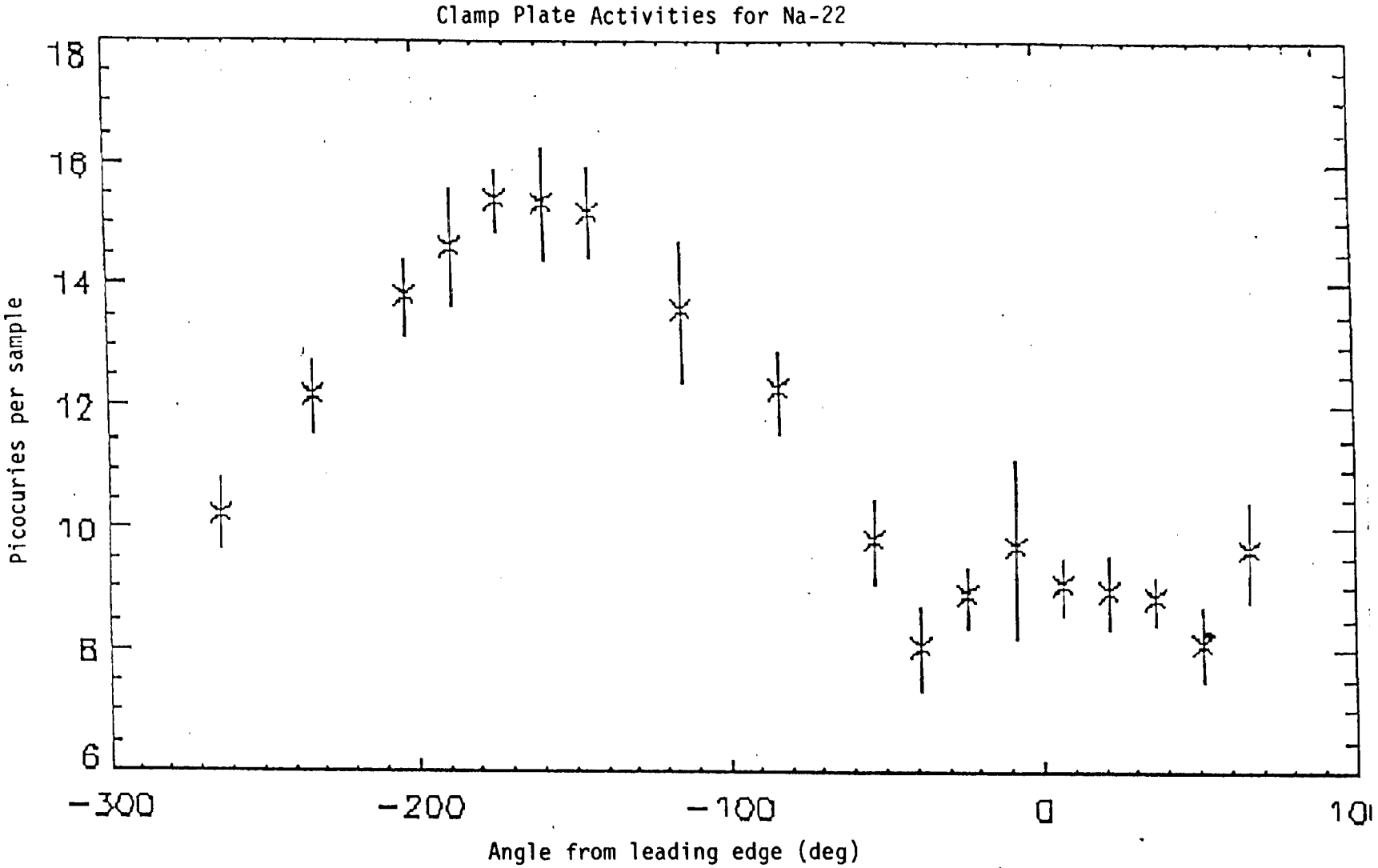

Figure 5. ^{22}Na activities for aluminum tray clamps taken from around the LDEF. The leading edge is 0 deg. and the trailing edge 180 deg. Activity is peaked at the trailing edge but found all round the spacecraft. As expected from the anisotropic cosmic ray and trapped proton fluxes, more activity is induced in materials on the westerly (trailing) side of the spacecraft.

EFFECTS ON LDEF EXPOSED COPPER FILM AND BULK

Palmer N. Peters
Space Science Laboratory, NASA/MSFC
Huntsville, Alabama 35812
Phone: 205/544-7728, Fax: 205/544-7754

John C. Gregory,* Ligia C. Christl,* Ganesh N. Raikar*
The University of Alabama in Huntsville
Huntsville, Alabama 35899
Phone: 205/895-6028, Fax: 205/895-6349

SUMMARY

Two forms of copper were exposed to the LDEF Mission 1 environment: a copper film initially 74.2 ± 1.1 nm thick sputter coated on a fused silica flat and a bulk piece of OFHC copper. The optical density of the copper film changed from 1.33 to 0.70 where exposed and the film thickness increased to 106.7± 0.5 nm where exposed. The exposed area appears purple by reflection and green by transmission for the thin film and maroon color for the bulk copper piece. The exposed areas increased in thickness, but only increase in the thickness of thin film sample could be readily measured. The increase in film thickness is consistent with the density changes occurring during conversion of copper to an oxide, however, we have not been able to confirm appreciable conversion to an oxide by x-ray diffraction studies. We have not yet subjected the sample to e-beams, or more abusive, investigations out of concern that the film might be modified.

*Work supported in part by grant from UAH Research Institute, and NASA grant NAGW-812 and contract NAS8-36645.

INTRODUCTION

The copper samples represent 2 of 64 cylindrical samples of 2.54 cm (1 inch) diameter that were flown on the leading, C9, tray of LDEF Mission 1 for 5 3/4 years of exposure in low Earth orbits. Matching trailing samples, which showed little effect, were located in the C3 tray. Appreciable effects on the copper were not anticipated, since active oxygen discharges on the ground for short periods had not shown the same gross degradation effects that silver had. The samples were mounted on ambient temperature surfaces believed to have had approximately room temperature values.

Copper oxide has a number of forms [1] ; two common forms of oxide are cuprite, Cu_2O, and tenorite, CuO. Cuprite has the properties: Molecular weight of 143.08, color is red, octahedral cubic structure, index of refraction of 2.705, and specific gravity of 6.0. The tenorite is black monoclinic, has a molecular weight of 79.54, index of refraction of 2.63, and specific gravity of 6.3 to 6.49. Copper has a molecular weight of 63.546, a cubic structure and a specific gravity of 8.92.

MEASUREMENTS

The copper samples were investigated by a number of techniques; these included: visual inspection by eye and optical microscope, photography, optical density measurements with visible white light using a scanning microdensitometer, thickness measurements by stylus profilometry, x-ray diffraction (XRD) electrical resistance measurements, ellipsometry, x-ray photoelectron spectroscopy (XPS), and profiling by optical interference techniques. We have not yet utilized scanning electron microscopy (SEM), Auger Electron Spectroscopy (AES), scanning Auger Microscopy (SAM), energy dispersive spectroscopy (EDS), or surface cleaning methods out of concern that we might modify the samples.

DISCUSSION

Visual inspection showed obvious changes to the exposed areas of both copper samples, as shown in Fig. 1. The bulk sample showed a maroon

discoloration, which did not change color with viewing angle, indicating that an interference film was not responsible for the color. The discoloration on the bulk sample was very-uniform in color. The thin film sample appeared basically purple when viewed off-normal and its reflectance and appearance were more poorly defined. By transmission the exposed area appeared green, and, while basically uniform, appeared to have small traces of inhomogenieties.

Optical densitometry measurements showed considerable changes in the optical density in the visible; the unexposed copper film had an optical density of 1.33 and the exposed area had an optical density of 0.70. The changes in optical properties appear to be too great to be attributed to contamination, and the fact that contaminants on the trailing surface produced minor optical changes compared to the ram direction supports a model involving atomic oxygen interaction.

The stylus profilometry measurements were practical only on the thin film sample, because the discoloration changes were relatively thin. Changes on the order of 10's and 100's of nm are difficult to measure at steps on surfaces unless the steps are very sharp and the surface is very flat. Neither of these conditions could be satisfied for the bulk copper sample; attempting to remove fine scratches of discoloration would also scratch the underlying copper; also, steps at the knife edges of the masking cover were not distinct enough to separate them from the uneven surface of the polished, but not flat copper disk. The thin copper film of 74.2 ± 1.1 nm initial thickness, however, was deposited on a fused silica flat and both the unexposed and exposed areas were easily scratched with fine lines near the mask boundary, exposing bare silica. The square negative pulse-like traces gave good indications of the thicknesses of exposed and unexposed regions at several locations around the mask perimeter. The average thickness in the exposed area was 106.7 ± 0.5 nm. Measurements at the mask edges gave a height of the step equal to an average of 34.3 nm, in agreement with the difference in total film thicknesses.

Using literature values [1] for the copper and its oxide and assuming that film expansion occurs normal and not lateral to the surface, we can estimate what should happen to film thickness if copper is converted to an oxide. Taking the reciprocal of the copper density and multiplying this by the molecular weight and dividing by Avogadro's number gives 1.183×10^{-23} cm^3/atom as an estimate for each atom. Since film densities are usually not exactly the same as bulk densities, this is only an

approximation, but taking the cube root of this value gives 2.28×10^{-8} cm, with which we can estimate the number of copper atoms in our 74.2 nm thick film, i.e. over a 1 cm^2 area we should have about 325 atomic layers and about 6.25×10^{17} copper atoms. One-half as many Cu_2O molecules can be formed from these copper atoms; thus, finding the cm^3/molecule for Cu_2O, as before, and multiplying by 3.13×10^{17} molecules gives 1.24×10^{-5} cm^3, or 124 nm thickness over the 1 cm^2 area. Similar calculation for CuO gives 129 nm over a 1 cm^2 area. Comparing these values to the measured value of 106.7 nm, indicates that partial conversion to either oxide would expand the copper sufficiently to give the measured value for the exposed material. X-ray diffraction results so far suggest free copper predominates both exposed and unexposed areas and only hints at the presence of Cu_2O, as shown in Fig. 2; however, these studies are very difficult because of the thinness of the film and further studies designed for thin films may improve the results.

Electrical resistance measurements were performed with two probe contacts at only a couple of locations, since soldering or outer bonding techniques were not allowed, and minimal contact with the surface was desired. Values of less than 100 ohms per square were obtained in the exposed area, which was orders of magnitude higher than in the unexposed area. No temperature dependent measurements to confirm metallic or semiconducting properties have been performed yet. Resistance calculation for a copper film 74.2 nm thick gives 0.23 ohms/square, which is also the order of accuracy of the two contact measurements used.

Ellipsometry measurements were attempted on the exposed surfaces with disappointing results; as with previous attempts to measure the optical properties of silver oxide, no definitive results were obtained. We have not determined the cause of the difficulty, but suspect overlying contamination and perhaps inhomegeniety in the film itself as possible reasons for failing to get good results.

XPS measurements were carried out using Mg Kα X-rays (1253.6 eV) as the excitation source. Three specimens (two thin films, C3-16 and C9-16, and one bulk, C9-30) were analyzed which showed varying degrees of surface contamination and the atomic concentrations of the all the species on these surfaces are shown in Table 1. Cu 2p core level was used to characterize the presence of Cu_2O and CuO in addition to X-ray excited Cu $L_{2,3}M_{4,5}M_{4,5}$ Auger lines. It has been shown previously [2 and references therein] that Cu $2p_{3/2}$ from CuO is relatively broad and is

accompanied by a satellite on the high binding-energy side at about 9 eV and is due to the multiplet splitting in the $2p^5 3d^9$ final state. The Cu $2p_{3/2}$ peak from Cu_2O has a single peak which is considerably narrower and closely resembles the peak from metallic Cu. On the bulk Cu sample we obtained Cu 2p peak resembling CuO in the exposed and metallic Cu in unexposed regions, respectively. However, on the thin film specimens, only single Cu $2p_{3/2}$ peak was obtained in both exposed and unexposed regions which may be construed as indicating the presence of pure copper or Cu_2O species on the surface. This is supported by x-diffraction results discussed above. The Cu $L_{2,3}M_{4,5}M_{4,5}$ Auger spectra of CuO and Cu_2O show distinct diffrerences and their spectral shapes are considerably different. This will be discussed in detail elsewhere [3].

Eventually partial cleaning of small areas of the surfaces may be attempted by low flux argon ion bombardment through apertures, enabling profiling the film thickness, but this partially destructive technique will be delayed until other approaches have been exhausted.

Profiling the surface by optical interference techniques works best when the whole surface has similar optical properties, with preferably high reflectance. The results on the two halves with greatly different optical properties were poor, compared to the mechanical stylus profiles.

Scanning electron microscopy and energy dispersive spectroscopy will eventually be tried on a turbo pumped SEM system and perhaps with limiting apertures again. While these techniques should provide very useful results, especially on an EDS system with thin window capable of analyzing oxygen x-rays, it is important to be cautious, since electron beams can polymerize some materials like pump oil and break some bonds in other materials. We wish to investigate the surfaces further before taking these steps.

While selective modification occurred only in the ram direction, expansion of the exposed film was consistent with partial conversion to an oxide, and other supportive evidence suggests that the copper was modified by heavy oxidation in the areas exposed to the orbital ram. We lack full confirmation that this is the cause at this time.

REFERENCES

1 : "Physical Constants of Inorganic Compounds", Handbook of Chemistry and physics, P. B87-89, 52 Edition (1971), Ed. Robert C. Weast, The Chemical Rubber Co, Cleaveland, Ohio

2 : J. Ghijsen, L.H.Tseng, J. van Elp, H. Eskes, J. Westerink, G.A.Sawatzky, and M. T.Czyzk, Phys. Rev. B38 (1988) 11322

3 : G.N. Raikar, J.C.Gregory and P.Peters (in preparation)

FIGURE CAPTION

Figure 1: Photograph of the bulk and thin film copper samples from C9 tray

Table 1

Atomic Concentration

Unexposed Region						
Element	Cu	O	C	Si	Na	Cl
C3-16	6	21	67	5	0	1
C9-16	3	21.5	66	9	0	0.5
C9-30	5.5	25	63	5	0.5	1
Exposed Region						
Element	Cu	O	C	Si	Na	Cl
C3-16	9	23	62.5	4	0.5	1
C9-16	4	37.5	44.5	14	0	0
C9-30	9	55	18.5	17	0	0.5

Fig. 1.

MEASUREMENTS OF EROSION CHARACTERISTICS FOR METAL AND POLYMER SURFACES USING PROFILOMETRY

Ligia C. Christl and John C. Gregory
The University of Alabama in Huntsville*
Huntsville, Alabama 35899
Phone: 205/895-6840, Fax: 205/895-6349

Palmer N. Peters
Space Science Laboratory, NASA/MSFC
Huntsville, Alabama 35812
Phone: 205/544-7728, Fax: 205/544-7754

SUMMARY

The surfaces of many materials exposed in low earth orbit are modified due to interaction with atomic oxygen. Chemical changes and surface roughening effects can occur which alter optical and other properties (ref.1). The experiment A0114 contained 128 solid surface samples, half of which were exposed on the front and half on the rear of LDEF. Each sample has been subjected to many analyses, but this paper will only describe the methods and techniques used to measure the changes in roughness, erosion depths and material growth using profilometry.

INTRODUCTION

The effect of atomic oxygen on materials is highly variable. No method of measuring the effects is optimum for all materials. We have developed several techniques found valuable in analyzing a wide range of materials, varying from minute effects on the level of atomic dimensions to heavily etched surfaces. One of the most effective techniques has been to utilize the measurement of etched steps at interfaces between exposed and unexposed, or masked, areas by stylus profilometry. Stylus profilometers typically measure the vertical displacement of a stylus (usually a fine pointed diamond) as it is scanned horizontally across the surface. Highly magnified vertical displacements are plotted against horizontal positions greatly exaggerating surface detail. This technique has the ability to measure a wide range of etch steps, from below 1 nm to 1 mm. For measurements below 1 nm it is essential that optically flat surfaces be used and that the steps be measurable over very short lateral distances. As shown elsewhere (ref.2), to produce etch steps over short lateral distances requires very thin masks, preferably thin film patterns resistant to atomic oxygen that are strongly bonded to the substrate being exposed, or at least knife-edged masks essentially in contact with the surface; these types of mask avoid structures which

* Work supported in part by a grant from UAH Research Institute and NASA grant NAGW-812 and contract NAS8-36645.

accurate measurements of the spikes or plateaus that form at locations of slower etch, and provides an estimate of the maximum etch depth.

Polymethylmethacrylate, PMMA, is a plastic which is readily etched by atomic oxygen, forming a large number of small spikes at the bottom of the etch and a large etch step, as shown in Figure 10, and Figure 11. Figure 10, was traced on a sample mounted on the ambient temperature plate and Figure 11 is for a sample mounted on a separate thermally isolated plate of semipolished aluminum. The purpose was to examine the etch rate as a function of temperature. The small increase in etch in Figure 11 may be due to slightly higher temperature of the hot plate sample. The smooth plateau at the right of the etched area in Figure 10 is due to an artefact caused by the stylus catching on the large etch step and dragging the sample a short distance; heavily etched samples need to be secured for this reason.

CONCLUSION

Stylus profilometry is a very effective non destructive or minimal scratching technique to measure roughness, erosion depth and material growth of metals, polymers and carbons exposed to the atomic oxygen.

We have demostrated that these instruments (Talystep and Talysurf), used in combination with some of the techniques mentioned (scratching, step and transition measurements), have a wide range of resolutions, from ~1Å to a few hundred microns.

Examples, like iridium film, show the reliability of the instrument, giving the same thickness value for the transition in any direction scanned.

Stylus profilometry, by indicating decreases, or increases, in film thicknesses enables interpretations of changes in optical density measurements, i.e. whether thinning of the film or an increase in thickness with optical property changes are responsible for optical density changes.

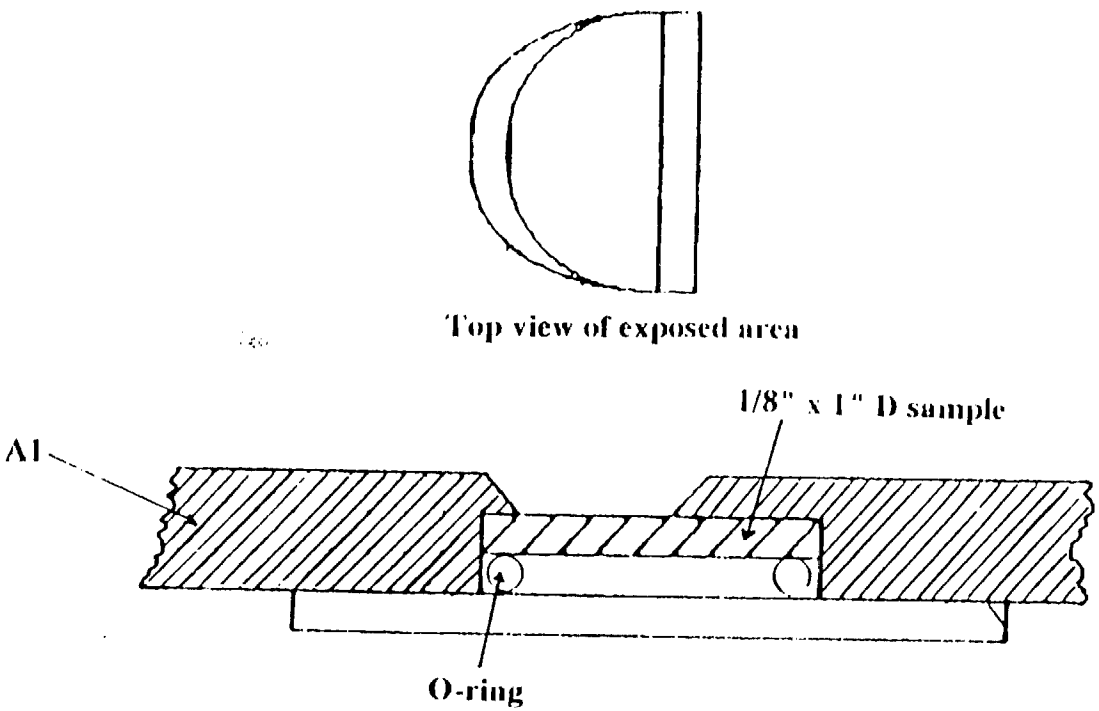

Figure 1. Cross-section of sample holder between exposed and unexposed areas

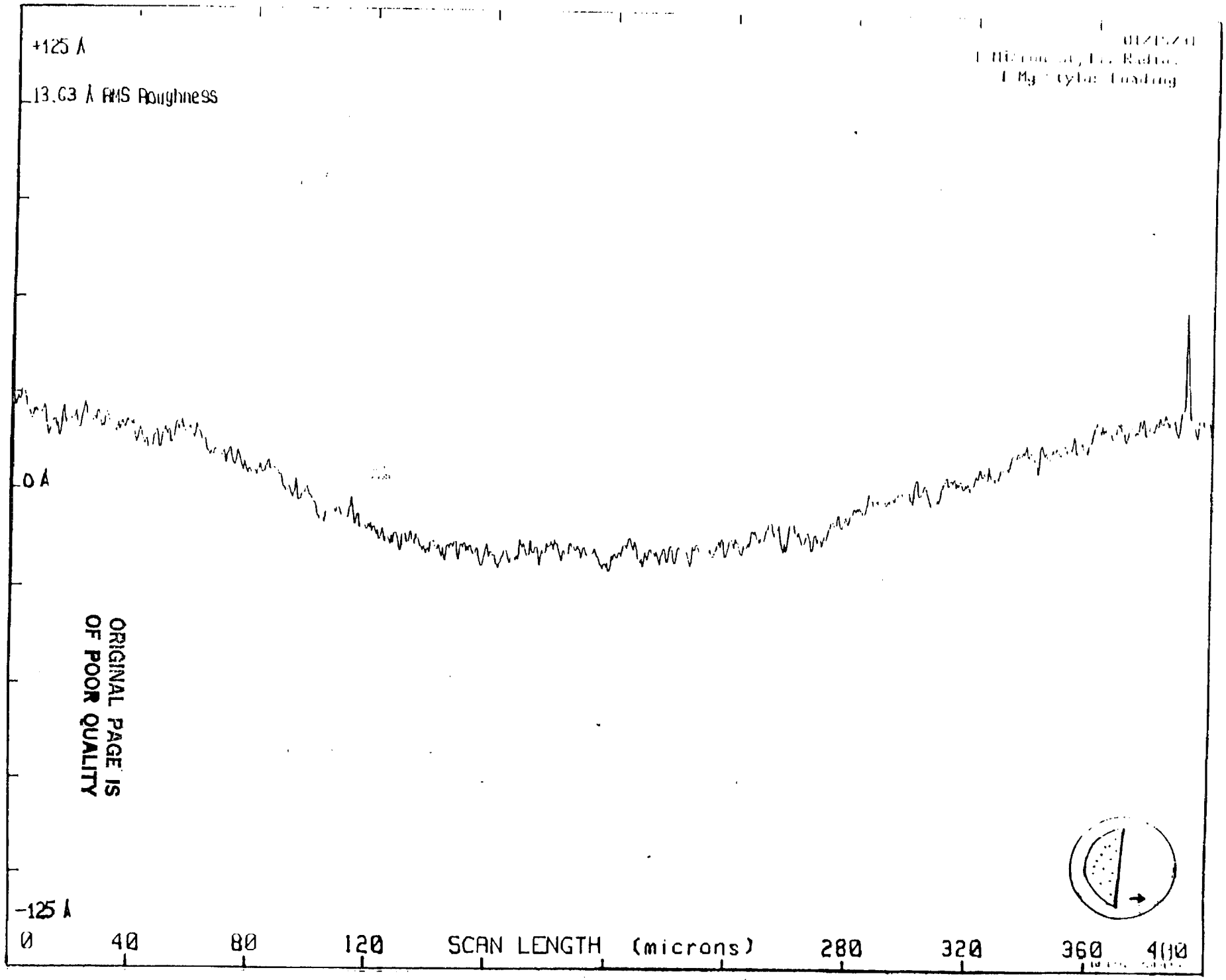

Figure 2. Surface profile of unexposed Iridium film

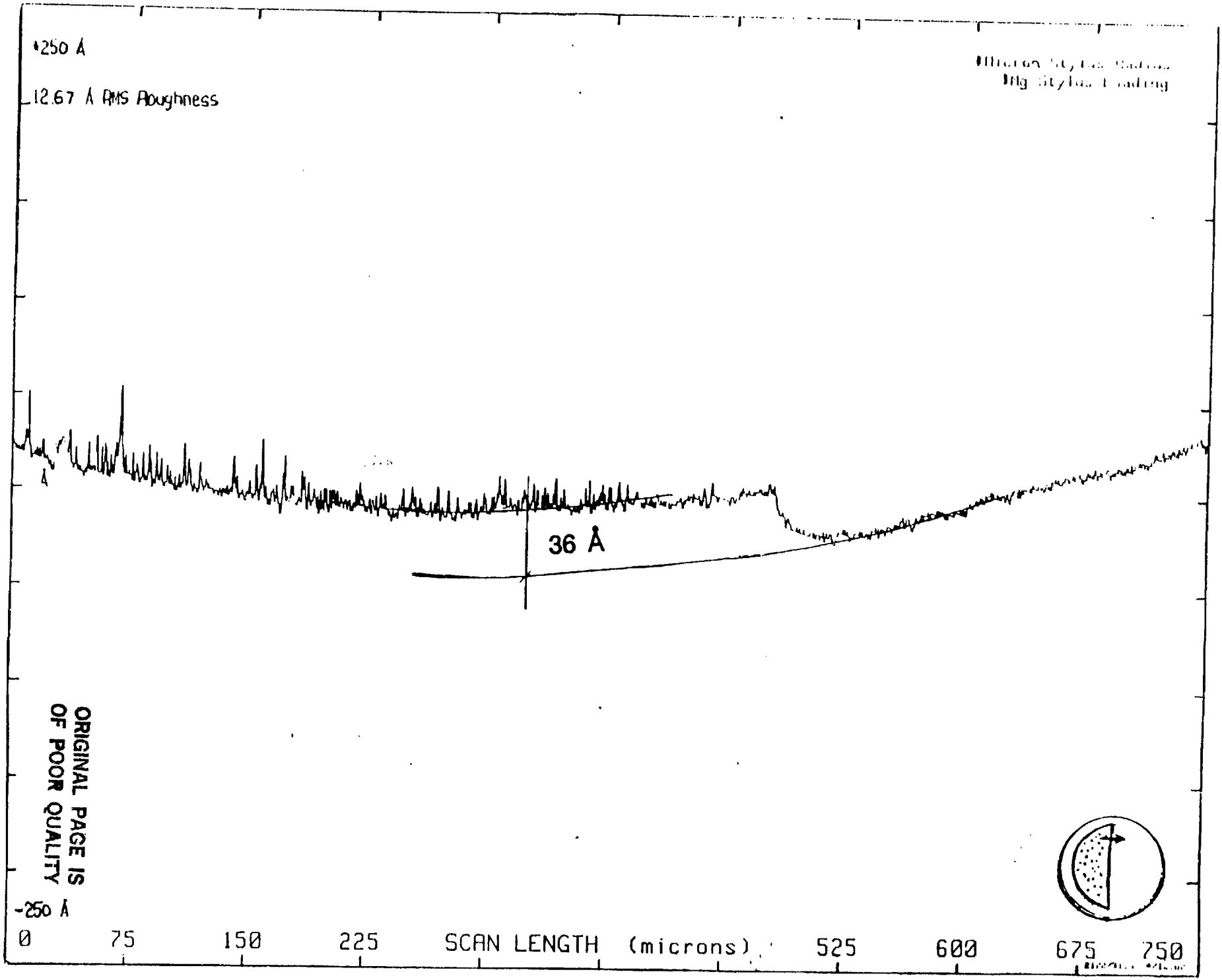

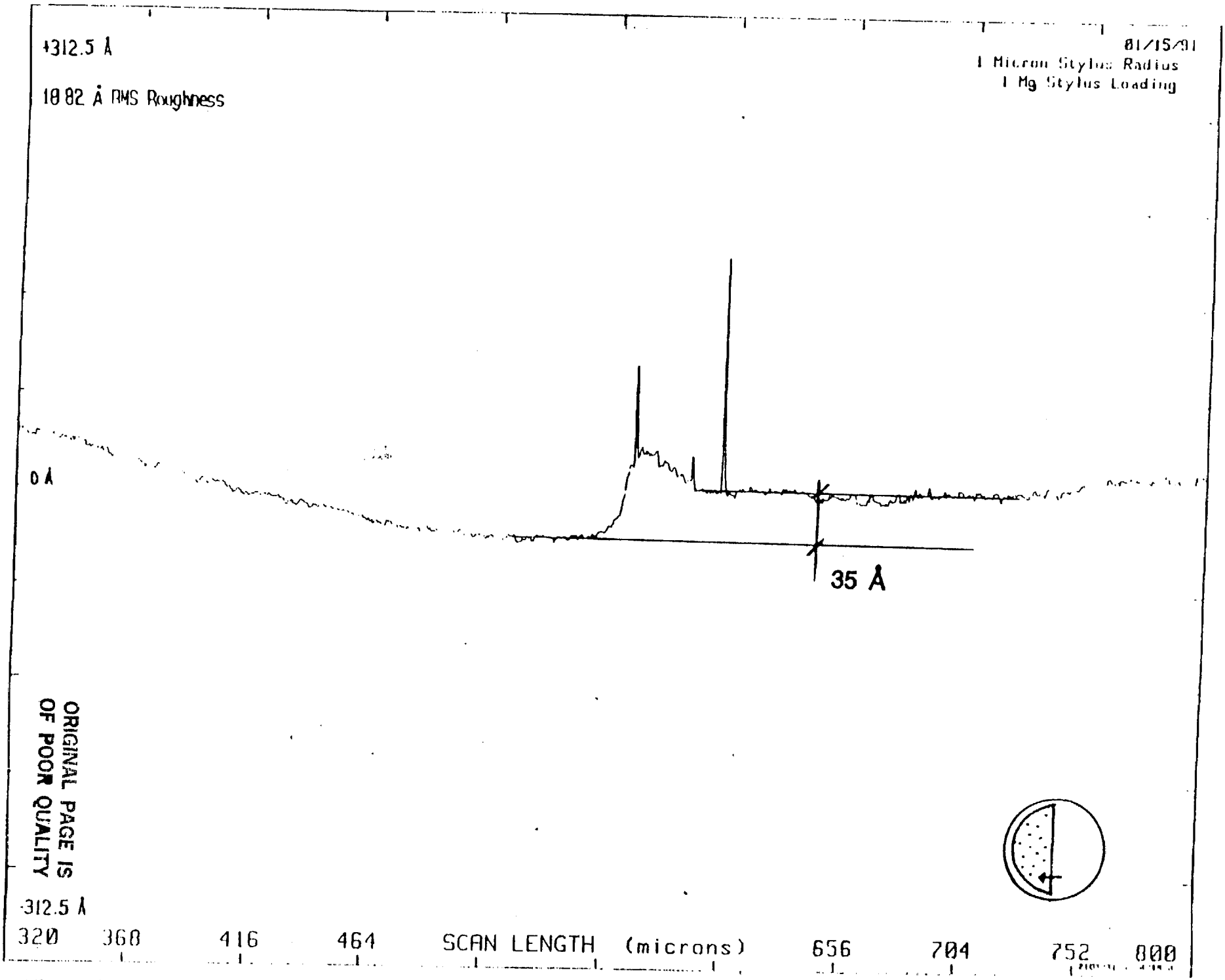

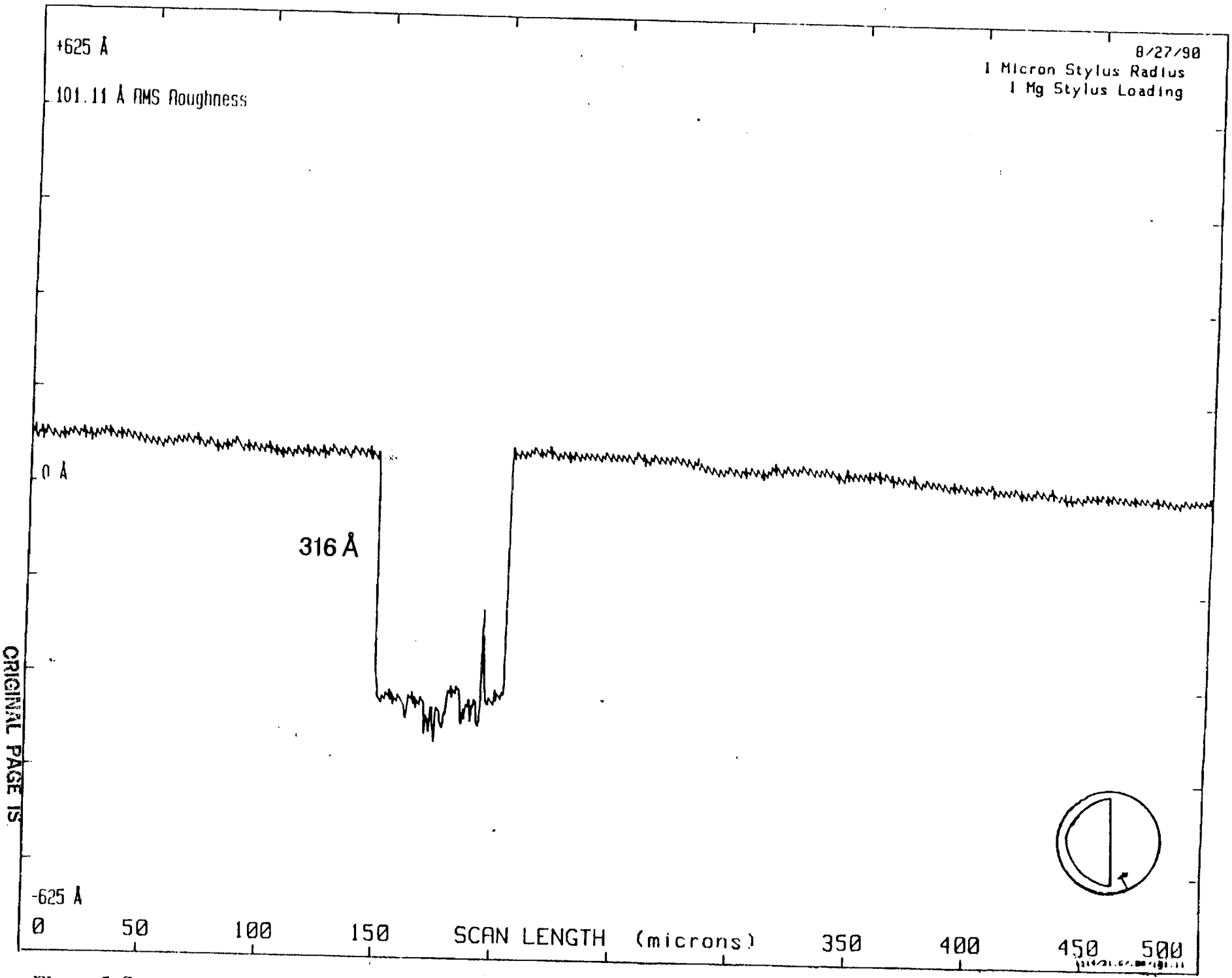

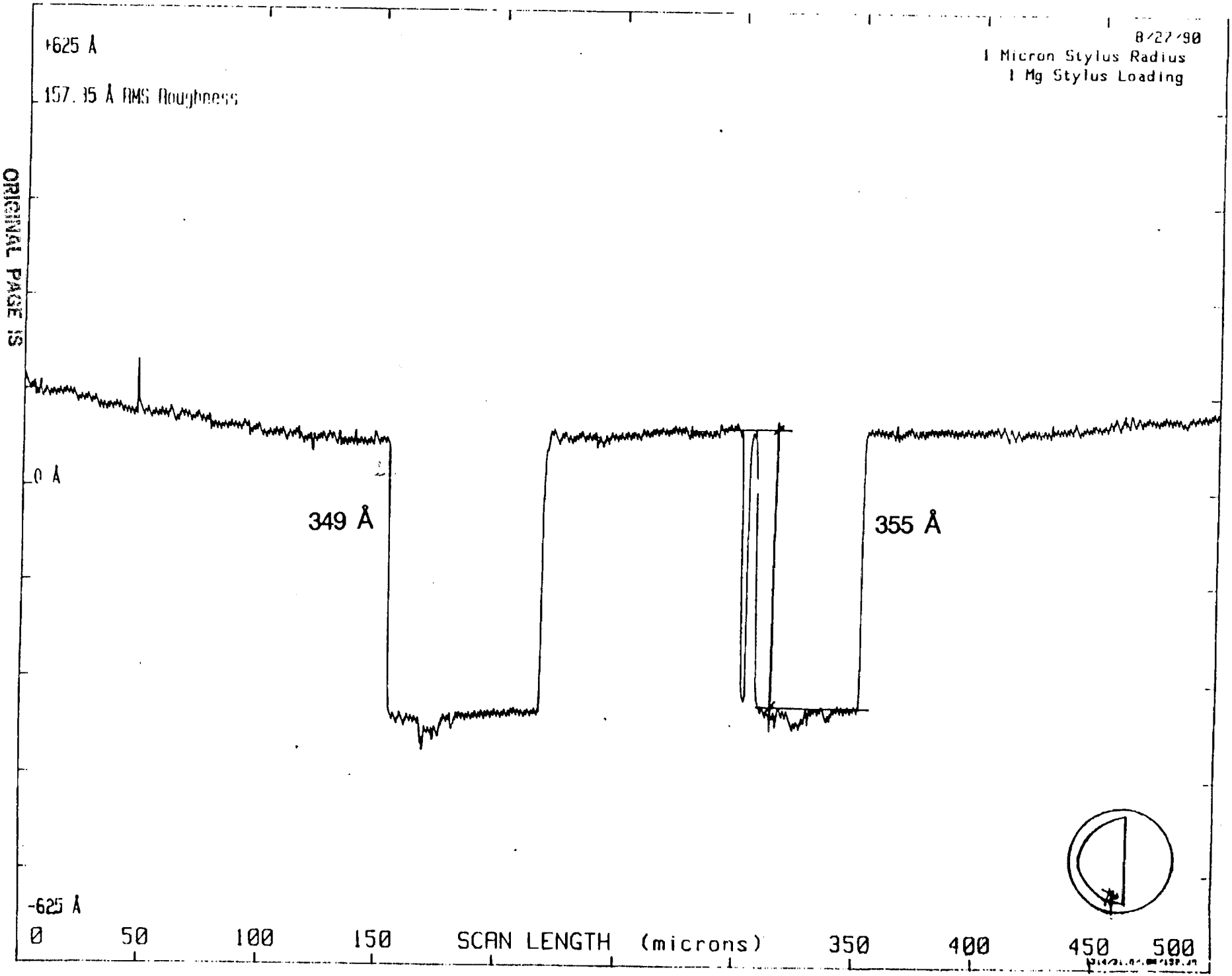

Figure 6. Surface profile of exposed Gold film

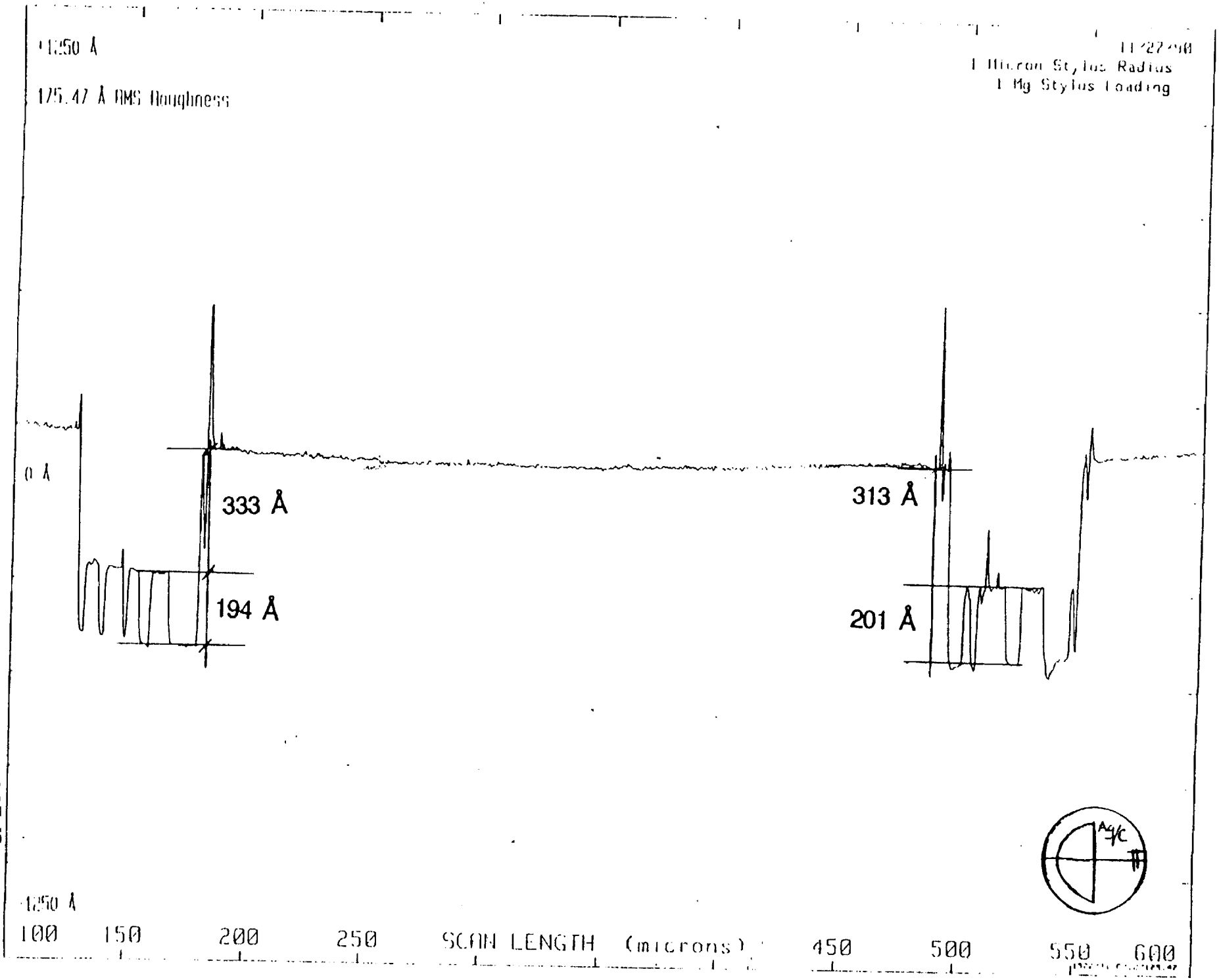

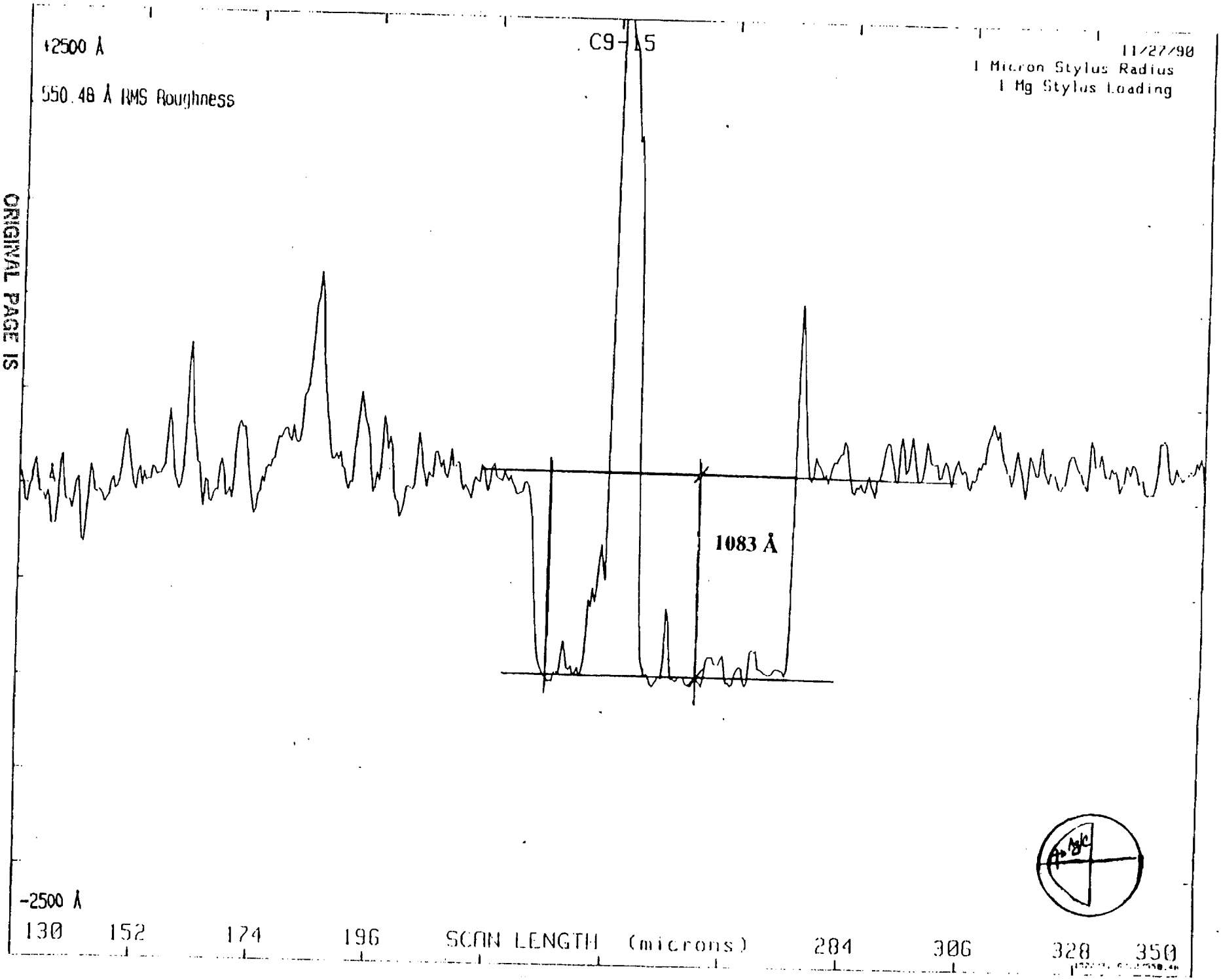

Figure 8 Surface profile of annealed Silver over Carbon film

Polycrystalline Carbon (C9-05)

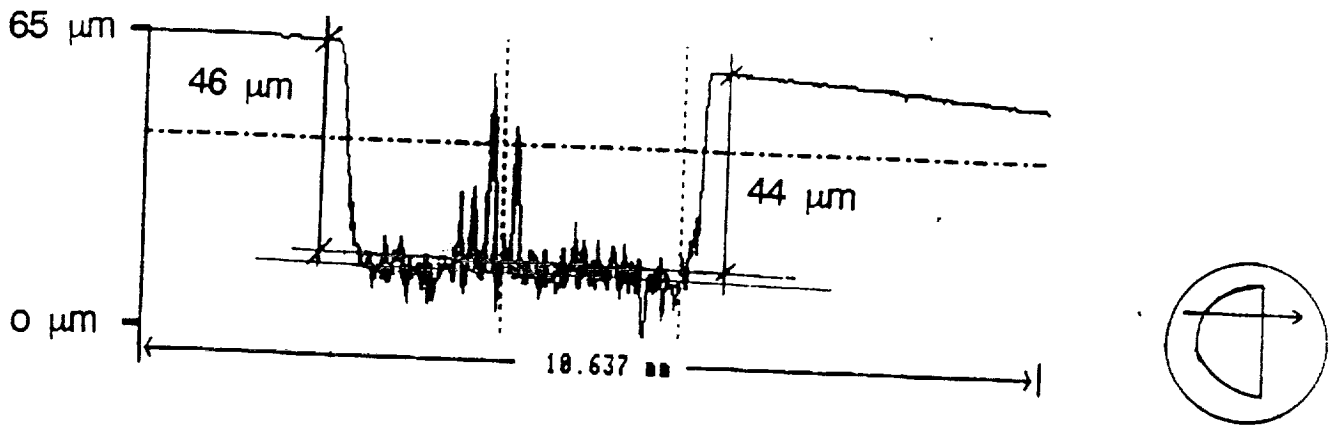

Figure 9. Surface profile of Polycristalline Carbon

PMMA (C9-31)

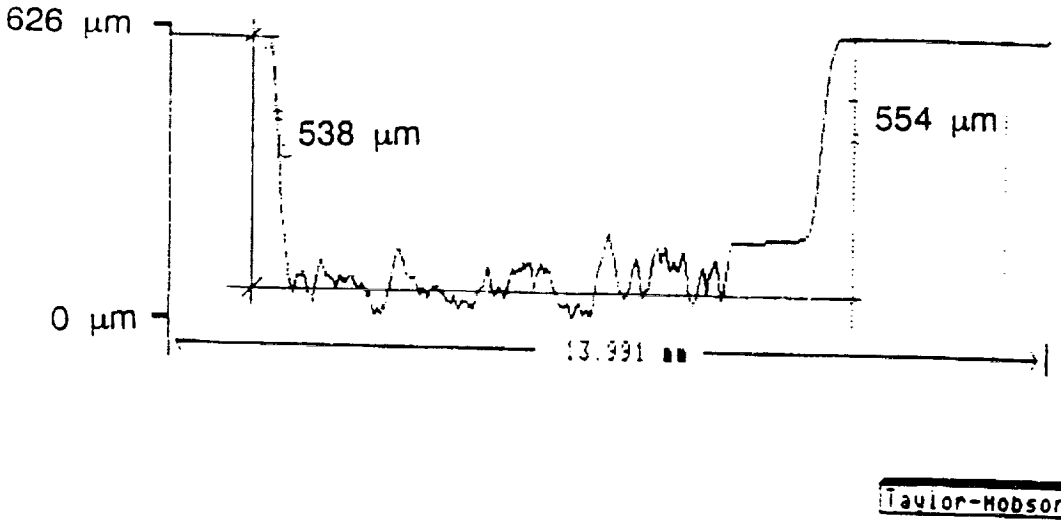

Figure 10. Surface profile of Polymethylmethacrylate at ambient temperature

PMMA (C9H-03)

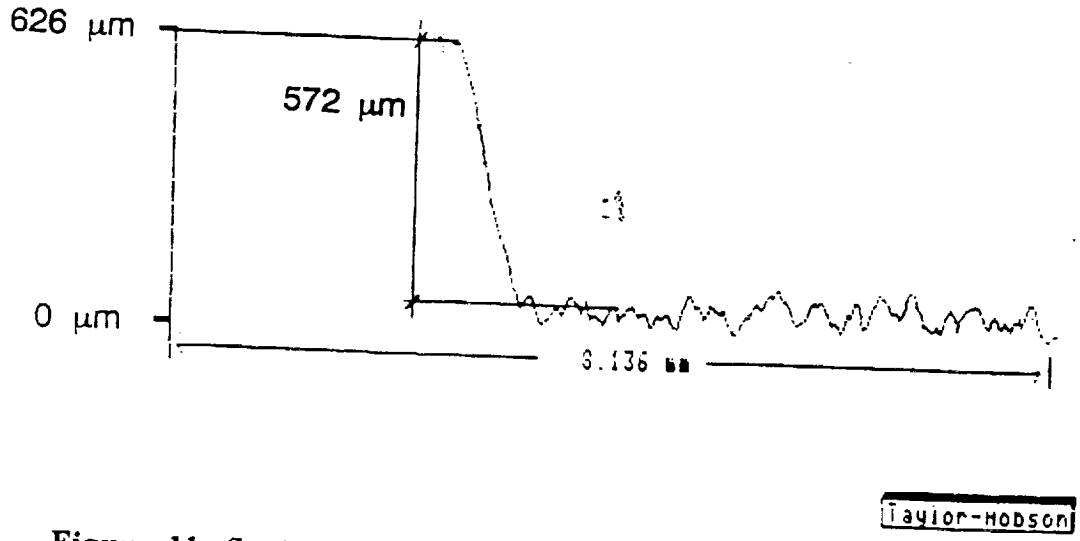

Figure 11. Surface profile of Polymethylmethacrylate at 10^0 C above the ambient temperature

PINHOLE CAMERAS AS SENSORS FOR ATOMIC OXYGEN IN ORBIT; APPLICATION TO ATTITUDE DETERMINATION OF THE LDEF

Palmer N. Peters
Space Science Laboratory, NASA/MSFC
Huntsville, Alabama 35812
Phone: 205/544-7728, Fax: 205/544-7754

John C. Gregory
The University of Alabama in Huntsville*
Huntsville, Alabama 35899
Phone: 205/895-6028, Fax: 205/895-6349

SUMMARY

Images produced by pinhole cameras using film sensitive to atomic oxygen provide information on the ratio of spacecraft orbital velocity to the most probable thermal speed of oxygen atoms, provided the spacecraft orientation is maintained stable relative to the orbital direction. Alternatively, as described here, information on the spacecraft attitude relative to the orbital velocity can be obtained, provided that corrections are properly made for thermal spreading and a co-rotating atmosphere. The LDEF orientation, uncorrected for a co-rotating atmosphere, was determined to be yawed 8.0° ± 0.4° from its nominal attitude, with an estimated ± 0.35° oscillation in yaw. The integrated effect of inclined orbit and co-rotating atmosphere produces an apparent oscillation in the observed yaw direction, suggesting that the LDEF attitude measurement will indicate even better stability when corrected for a co-rotating atmosphere. The measured thermal spreading is consistent with major exposure occurring during high solar activity, which occurred late during the LDEF mission.

INTRODUCTION

A requirement to study the LDEF attitude was identified and a pinhole camera was developed for this purpose as part of Experiment A0114 (refs. 1-3). The atomic oxygen sensitive pinhole camera uses the fact that oxygen atoms dominate the atmosphere in low-Earth orbits, and formation of a nearly

---

*Work supported in part by a grant from UAH Research Institute and NASA grant NAGW-812 and contract NAS8-36645.

collimated beam of oxygen atoms passing through a pinhole in a satellite front surface occurs as a result of the orbital velocity being greater than the most probable Maxwell-Boltzmann speed of the oxygen atoms. Thus, the range of incidence angles of atoms to satellite surfaces is very limited, as shown by the angular distribution curves for two different temperatures in fig. 1 and described in greater detail elsewhere (ref. 4). The same maximum oxygen atom intensity was used for both temperatures to illustrate how the intensity spreads into the wings for higher temperatures. A thin film of material (silver in this case), which is sensitive to atomic oxygen, then forms an image of the impact spot.

The temperature of the thermosphere depends upon solar activity; the 700 K temperature in fig. 1 is characteristic of a solar minimum and the 1500 K is closer to a solar maximum. LDEF altitude was high during the solar minimum of September 1986 (initially deployed at 480 km in April 1984) where oxygen density was lower and had decayed by the time solar maximum was reached in June 1989 (recovery occurred at 310 km in January 1990). Most of the exposure in the pinhole camera, occurred close to solar maximum when the altitude was lower, the oxygen density was greater, and the angular distribution for atom incidence was widest. As will be described later, a well-defined spot was measured on the pinhole camera's silver sensor surface. Although overall darkening from overexposure (scattered atoms within the camera) was observed, this spot has been interpreted as being from the direct incidence beam and was used to determine the orientation of the LDEF relative to the orbital velocity.

MEASUREMENTS

The pinhole camera consisted of a 0.3 mm thick stainless steel hemisphere 3.25 cm (1.28 in.) radius, polished on the concave surface and coated with vacuum-evaporated silver. Silver was used because it discolors from formation of oxide (ref. 5). The pinhole had a conical shape with an included angle much wider than the maximum atom incidence angle and terminated as knife edges at a pinhole diameter of 0.5 mm (0.020 in.). The pinhole was positioned at the center of the silvered hemisphere. As shown in fig. 2, the exposure at any point on the hemisphere will depend upon the solid angle subtended by the pinhole from that point and the point's angular displacement from the orbital direction, i.e., the atom fluence as a function of angle from the velocity vector as shown in fig. 1. For orientations within 10° of the orbital direction, the solid angle subtended by the pinhole is constant within 2%; the predominant effects of pinhole size and thus solid angle are to reduce the overall fluence, or exposure, and increase resolution by reducing pinhole size.

Thus, the spot produced behind the pinhole should be centered with the LDEF's velocity vector and the spot's intensity should correspond to the distribution shown in fig. 1. Any variation in the attitude of the LDEF's velocity vector relative to the atmosphere would cause the spot to wander, producing a nonspherical, larger than normal, spot compared to that produced by thermal spreading of the beam.

Two techniques were used to determine the spot center and its shape: the first technique involved measurements taken directly from an enlarged photograph of the hemisphere taken on-axis with a 120 mm format camera and a 80 mm macro lens, and the second technique involved digitizing a 512 x 512 pixel CCD video camera image of the hemisphere and processing it to obtain both the spot and hemisphere centers and the spot geometry. Both techniques gave similar results.

DISCUSSION

Assuming that misalignment of the pinhole camera relative to the LDEF frame was negligible (machined surfaces and robust structures offer assurance of this), an LDEF orbiting with nominal attitude should have produced a spot centered on the hemisphere and uniformly round. The actual spot, as shown in fig. 3, was off-center, as would be produced by $8^\circ \pm 0.4^\circ$ clockwise yaw viewed from the space end. The spot was elliptical (major axis 14.8° and minor axis 14.1°, as subtended from the pinhole), with the major axis in the satellite yaw direction. It is noted that a yaw of 8° should have narrowed the spot in the yaw direction, not widened it as observed; thus, an oscillation in atom incidence along the yaw direction is the likely cause. This originally led us to conclude that the LDEF oscillated in the yaw direction (i.e., about its long axis), but it has been brought to our attention (Bourrassa, private communication, 1990) that a co-rotating Earth's atmosphere interacting with an inclined orbit produces an oscillation in the angle of incidence of oxygen atoms at the surface. We have verified that the oscillation occurs in the yaw direction, as observed, but the maximum range should be about $\pm 1.5^\circ$, not the estimated $\pm 0.35^\circ$ obtained from the ellipticity measured on the spot. While the center of the spot is rather well defined and is believed to be the average orientation for the LDEF, oscillations, thermal spreading, and other influences on exposure, such as multiple scattering must be separated. Some considerations are:

1. The exposure of the silver was an integrated effect which occurred over 5 3/4 years, over a wide range in oxygen atom temperature, and with an excess background from multiply-scattered atoms. However, most of the oxygen exposure was received during the last six months of the flight.

2. We have not been able to depth profile the exposed silver film, particularly across the spot. Although a nearly circular bulleye pattern suggests a profile similar to those in fig. 1, we have not yet devised a satisfactory technique for measuring optically opaque profiles.

3. Without a depth-composition profile it is not possible to fit the oxygen exposure to a known temperature distribution and there is some uncertainty as to the exact limits of the spot diameter (i.e., where the spot ends and the background takes over); however, it appears that rings on the spot represent equal thicknesses of oxide and provide the measured ellipticity. The minor axis of the spot could represent temperatures as high as 1500 K if assigned FWHM in fig. 1.

4. An oscillating structure and the apparent oscillation caused by an inclined orbit and rotating atmosphere do not yield the same angular flux distribution in a pinhole camera. An oscillating structure sweeps rapidly through the zero displacement and pauses at the extreme angular displacement; The opposite is true for the rotating atmosphere effect. Thus, a mechanical oscillation has a larger integral effect on spot diameter for the same number of degrees of oscillation. We are calculating these profiles with atmospheric oscillations included. Further study is needed to accurately determine the LDEF's range of oscillation.

Analysis by x-ray diffraction of the black powder flaking from much of the camera interior confirmed that it was Ag_2O. For reasons yet unknown, the primary exposed spot was more stable than the rest of the background exposed surface; this assisted our investigation.

AKNOWLEDGEMENTS

The authors are grateful for continued assistance from David Carter, William Kinard, and Jim Jones of the NASA Langley Research Center; to Howard Foulke of the General Electric Company for explanations of their satellite stabilization studies; to William Witherow for digital image measurements; and to Charles Sisk for computer assistance.

REFERENCES

1. Clark, L. G., Kinard, W. H., Carter, D. J., and Jones, J. L., Jr., Eds., "The Long Duration Exposure Facility (LDEF): Mission 1 Experiments," NASA SP-473, Scientific and Technical Information Branch, NASA, Washington, D.C. (1984).

2. Siegel, S. H. and Das, A., "Passive Stabilization of the LDEF," Final Report on contract NASI-13440, GE Document No. 74SD4264, November 1974, General Electric Company, Astrospace Division, Philadelphia, PA.

3. Siegel, S. H. and Vishwanath, N. S., "Analysis of the Passive Stabilization of the LDEF," GE Document No. 78SD4218, August 1977, General Electric Company, Astrospace Division, Philadelphia, PA.

4. Peters, P. N., Sisk, R. C., and Gregory, J. C., "Velocity Distributions of Oxygen Atoms Incident on Spacecraft Surfaces," J. Spacecraft and Rockets, 25(1), 53-58 (1988).

5. Thomas, R. J. and Baker, D. J., "Silver Film Atomic Oxygen Sensors," Can. J. Phys., 50, 1676 (1972).

FIGURE CAPTIONS

Fig. 1. Intensity of oxygen atoms versus incidence angle, cap-theta, in degrees from the orbital ram direction for two equilibrium temperatures of the atoms.

Fig. 2. Schematic of pinhole camera with off-centered spot due to yaw of the LDEF and showing thermal spreading about the spot center due to the effect shown in Fig. 1.

Fig. 3. Photograph of exposed silver hemisphere from pinhole camera; overall dark flaking area is interpreted as overexposure from multi-scattered atoms, and the spot, which is more stable, is believed to be from direct incidence.

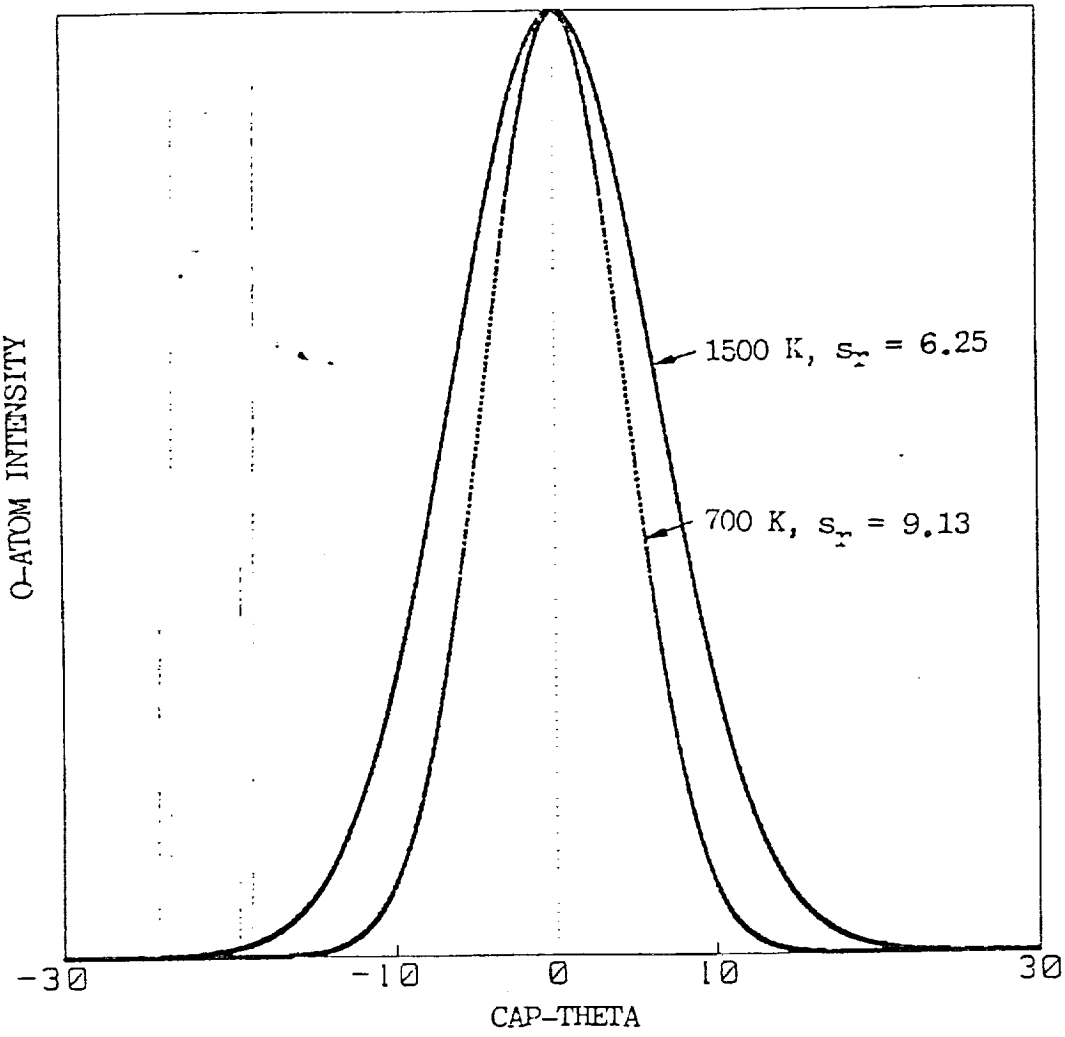
O-ATOM INTENSITY
1500 K, s_x = 6.25
700 K, s_x = 9.13
-30
-10
0
10
30
CAP-THETA

Fig. 1

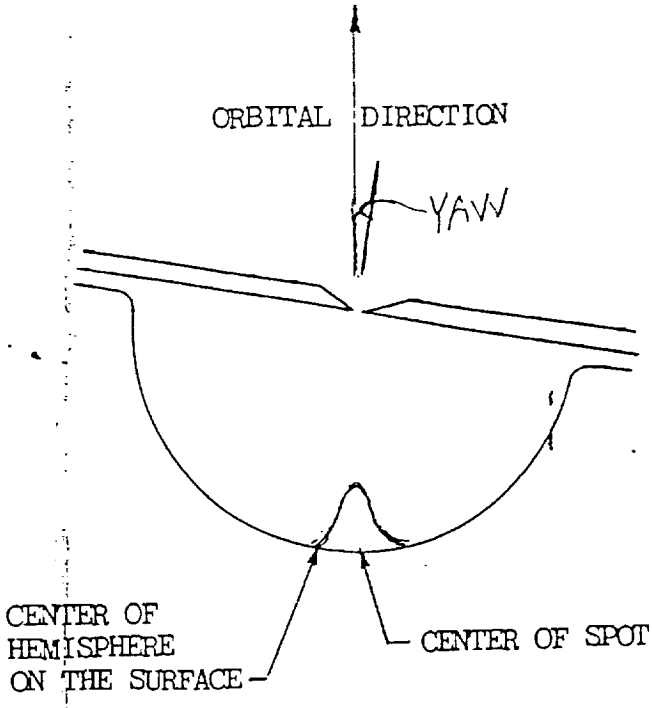

Fig. 2

Fig. 3